TRANSPORTATION TECHNOLOGY CENTER, INC.
TECHNOLOGY DIGEST
JULY 2021
TD21-017

The research described was performed by Transportation Technology Center, Inc., a wholly owned subsidiary of the Association of American Railroads.

Wheel Defect Detection Using Electromagnetic Acoustic Transducers

Anish Poudel, Brian Lindeman, Matthew Witte, and Gary Fry

Key Findings:

- The off-the-shelf EMAT sensor demonstrated excellent detection capability with good signal-to-noise-ratio (SNR) for the wheel samples provided. The results suggest the EMAT is capable of detecting internal wheel defects.
- The EMAT does not require a liquid couplant nor contact with the inspection subject, which could be advantageous for an in-motion cracked wheel detection system.
- Signal noise in a defect-free area was typically not more than 3 to 5 percent full-screen height (FSH); whereas defects validated through a destructive evaluation showed signals of at least 50 percent FSH.
- The minimum SNR was 5:1 but was typically higher in most cases throughout the trials. If calibrated at 4:1 SNR, the EMAT sensor would most likely pick up all of the defects in the test wheel samples.
- TTCI is currently working with Innerspec to demonstrate this technology using array EMAT sensors for in-motion inspection.

Working with Virginia-based Innerspec Technologies, Inc. (Innerspec), TTCI tested the capability of electromagnetic acoustic transducers (EMATs) nondestructive evaluation (NDE) technology for detecting internal defects in railroad wheels. This proof-of-concept study used an off-the-shelf EMAT sensor in a static laboratory environment. TTCI demonstrated a favorable signal-to-noise-ratio (SNR) capability for detecting internal wheel defects with the EMAT sensors. Defects in the test wheel samples that were unspecified prior to testing were accurately identified with the EMAT sensors. The ultimate goal of this research is to help facilitate in the development of EMAT technology as an alternative in-motion automated cracked wheel detection system (ACWDS) suitable for implementation in railroad revenue service.

BACKGROUND

Railroad wheels are subject to wear and fatigue during service. Surface defects and shallow internal cracks below the tread surface can form as a result of cyclic mechanical loading. Wheels are inspected regularly and removed from service when they exceed the Association of American Railroads' (AAR) specifications for condemnable defect criteria as defined by Rule 41 of the AAR *Field Manual of the AAR Interchange Rules*.[1] Railroad wheel condition is primarily assessed through visual inspection and wayside detectors; e.g., wheel profile measurement system, wheel impact load detectors (WILD), and machine vision systems. These inspection approaches, however, cannot detect internal fatigue cracks until the cracks reach the surface and cause a visible geometric feature. Many broken wheels fail before exhibiting high impacts (80 kips or higher) as measured by WILD systems.[2] Manual NDE processes such as hand-held ultrasonic inspections, although effective, are extremely labor-intensive and require a substantial time commitment. For these reasons, recent research efforts, such as the one described in this *Technology Digest,* have focused on in-track inspection systems that can automatically detect internal fatigue cracks in wheels on moving trains.

EMAT PRINCIPLE

The EMAT is an ultrasonic testing (UT) NDE method that does not require a couplant to perform the inspection as the ultrasound is generated directly within the material adjacent to the transducer.[3] The EMAT ultrasound generation is based on the interaction between the magnetic field created by a magnet and the eddy currents induced in the test piece by a coil circuit. The combination creates a Lorentz force within

the material, which causes vibrations of the material's lattice and thereby generates ultrasonic waves. Figure 1 shows a comparison of the EMAT UT principle with the conventional piezoelectric-based UT principle. Depending on the sensor design, the wave type and wavelength can be varied. The same or similar sensor receives a return signal and provides a very precise measurement of the propagation velocity of those waves in the test piece.

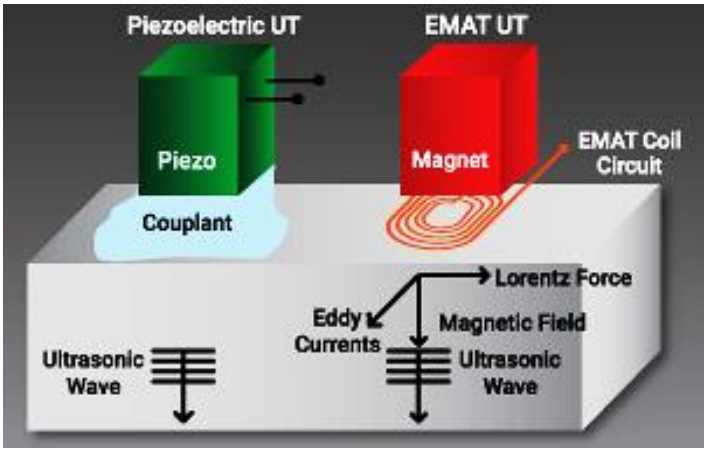

Figure 1. Schematic showing differences between conventional and EMAT UT generation principles

One of the main limitations of UT inspection is the inability to inspect the area just beneath the surface of the test material often referred to as a "blind zone." There is typically a strong pulse of energy that lasts for a few microseconds during which the receiver is saturated and cannot receive the signal. During this time the ultrasonic signal is still traveling through the material, but the receiver is "blind."

In piezoelectric transducers, one way to avoid this blind zone is to use a delay line (an extension of the transducer). The delay line allows the blind zone to be inside the extension, and therefore the instrument can more accurately measure near the surface of the inspection subject. With a delay line, the gate is positioned immediately after the interface echo, and it allows the instrument to detect defects as close as 2 mm from the surface.

If a delay line is not used, as in a contact transducer, the typical blind zone is approximately 2 to 3 μs (the time of flight for the return trip), which is equivalent to 0.23 to 0.345 inch. It is not possible to use a delay line with EMATs because the sound is generated in the inspection subject. For EMAT sensors, the typical blind zone is between 2 to 4 μs (0.128 to 0.256 inch). However, defects that are greater than 3 to 4 mm in depth can be seen by subsequent reverberations of the signal in the EMAT approach. These reverberations are caused by the sound bouncing back and forth between the defect and the surface of the material. In order to measure the actual depth of shallow defects in the blind zone, the standard approach for the EMAT is to measure the distance of the peak-to-peak amplitude on these reverberations using special algorithms.

TEST SETUP

TTCI provided cut sections from two Class C wheels (identified as W-56 and W-41) for testing at the Innerspec laboratories. Each wheel sample contained internal sub-surface fatigue cracks. TTCI determined the locations of the internal defects using conventional UT handmapping, but did not mark the wheels or reveal the defect locations to Innerspec. A single-channel, off-the-shelf EMAT sensor was used for the feasibility demonstration. Figure 2 shows the EMAT static test setup in the laboratory.

Figure 2. Single channel EMAT test setup

The tests were conducted using the Innerspec PRIMO-SC EMAT test equipment, and a Wi-Fi enabled tablet displayed the results. The EMAT sensor was operated in normal beam shear wave mode at a center frequency of 1,500 kHz. This proved to be sufficient to penetrate the steel wheel material. Since the velocity of shear waves is approximately half that of longitudinal waves, the wavelength of this transducer is similar to a 3 MHz longitudinal wave piezoelectric-based ultrasonic transducer. For future test systems, the EMAT sensor design would need to be optimized for enhanced performance and optimal coverage.

RESULTS

A-scans (amplitude versus time/distance plots) were captured at various points in the wheel samples to demonstrate the signal quality. Initial EMAT tests revealed that wheel sample W-41 had sub-surface fatigue cracks concentrated in the band along the center of the tread. Wheel sample W-56 also showed defect indications, but fewer in number, and the ultrasonic reflections were not as strong as those in wheel sample W-41. The wheel samples were cut flat, making the middle area thicker than the

sides. The flat part limited the depth of the scan due to the backwall signals moving closer to the defect indications at the shallower depths. Detected defects were marked with tape and labeled on each wheel sample. Figure 3 shows the defect annotations on wheel samples W-56 and W-41 as identified during the EMAT evaluation and labeled in white paint stick markings. Additional annotations have been added to these photos using a yellow font to further highlight the EMAT alphabetic defect locations and to indicate the numeric defect locations resulting from the UT handmapping on W-56. UT handmapping indicated a single long defect on W-41 not labeled in Figure 3. Table 1 shows conventional UT handmapping test results on both wheel samples.

Figure 3. EMAT-detected defects on wheel cut out samples

Table 1. Hand-UT characterization results for wheel samples

Wheel ID	Defect ID	Distance from the Rim Face	Length	Width	Depth
W-56	1	2.20″	0.30″	0.25″	0.27″
	2	2.30″	0.70″	0.25″	0.22″
	3	2.20″	0.50″	0.25″	0.28″
W-41	1	1.90–2.70″ (A-end) 2.20–2.80″ (B-end)	17.00″	0.60-0.80″	0.13-0.28″

Figure 4 is an example A-scan result on a clean, defect-free area of wheel sample W-56. The defect alarm gate for the ultrasonic signal was set at the 4:1 SNR as represented by the green line segment that starts around a 0.5-inch depth. This signal gate is around 1.1 inches in length. Ultrasonic calibration was conducted at 80 percent of the full screen height (FSH). The 4:1 SNR corresponds to 20 percent FSH of the recorded ultrasonic signals. Nowhere does the signal waveform cross over this gate or line. Strong reflections to the left of the green segment represent the near-surface noise. The backwall reflection occurred at a depth of 1.7 inches and had an ultrasonic reflection/strength of about 6 percent FSH. The noise level in the A-scan was approximately 3 to 5 percent FSH.

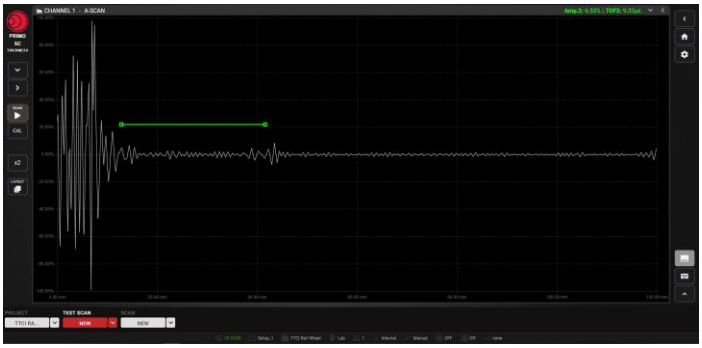

Figure 4. A-scan snapshot at clean, defect-free area, sample W-56

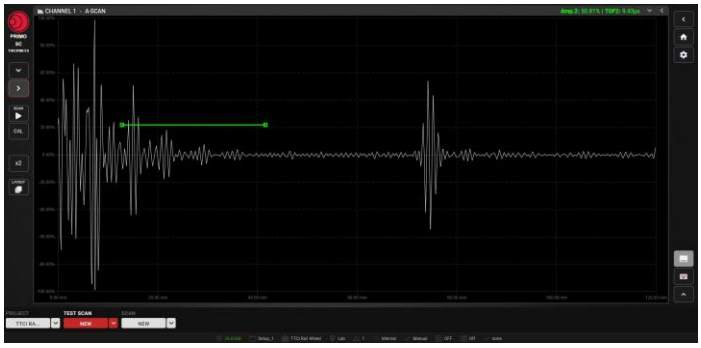

Figure 5. A-scan snapshot from spot "A," sample W-56

Figure 5 shows an example A-scan result from the spot marked "A" on the wheel sample W-56. The defect signal crosses the threshold of the ultrasonic gate at a depth of approximately 0.6 inch with the ultrasonic signal reflection of about 50 percent FSH. The backwall reflection is located about 2.9 inches deep and, in this case, can be considered strong because it is roughly the same magnitude as the defect reflection. In addition, the ultrasonic reflections at the other locations "B," "C," and "D" in wheel sample W-56 were about 80, 70, and 50 percent FSH, respectively. However, the ultrasonic reflection at location "E" barely crossed 20 percent FSH and had a different signal feature which, most likely, was due to the surface tread condition in that location. Similarly, on wheel sample W-41 strong reflections were observed—near 100 percent FSH at the spots labeled A, B, and E

and 60 percent FSH at spots C and D. The depths of reflection varied slightly but the SNR was again greater than four in all locations. As expected, the reverberations were clear from all defects evaluated in this proof-of-concept study, but the X-axis of the A-scans does not represent the actual depth of detection. For an in-track wheel inspection system, the pulse and sensor configurations could be optimized to reduce the effect of the blind zone, and depth estimation algorithms (based on reverberations) could be used to provide accurate depth measurements for defects found within the blind zone.

Defect verification was also conducted using destructive testing, i.e., by slicing the wheel samples at the locations identified by the EMAT. Table 2 shows the findings, and Figure 8 shows images of the defects.

Table 2. Destructive characterization results for NDE verification

Wheel ID	UT hand map defect ID	EMAT defect ID	Distance from the rim face	Width	Depth
W-56	1	A	2.13"	0.13"	0.25"
	2	B	2.25"	0.19"	0.25"
	2	C	None Found		
	3	D	2.50"	0.19"	0.06"
	N/A	E	None Found		
W-41	1	A	2.13"	0.25"	0.19"
		B	2.31"	0.25"	0.13–0.19"
		C	2.25"	0.38"	0.13"
		D	2.06"	0.50"	0.13"
		E	2.06"	0.38"	0.13"

W-56 "A" W-56 "B"

W-41 "A" W-56 "B"

Figure 8. Destructive verifications on EMAT findings, wheel samples

Destructive analysis confirmed the EMAT findings except for locations C and E in the W-56 wheel sample. Destructive analysis findings from the location C did not reveal any defects; however, both NDE approaches determined a sub-surface crack at this location. As discussed, location E barely met the EMAT criteria for a defect and was likely the result of the surface tread conditions.

CONCLUSION

EMAT off-the-shelf sensor technology demonstrated excellent detection capability with good SNR for the wheel samples provided. The result suggests capability to detect wheel defects. The EMAT technology can be adapted for complete wheel inspection with a sensor array to cover the complete width of the tread and wheel circumference in order to perform in-line high speed inspections without the need for couplant handling and delivery systems, as required for piezoelectric-based ultrasonic inspection systems. However, the effect of instrument lift-off (sensor-to-wheel tread distance) must also be understood. TTCI is currently working with Innerspec to demonstrate this technology using array EMAT sensors for in-motion inspection. Results will be reported in a future issue of *Technology Digest.*

References

1. *Field Manual of AAR Interchange Rule*s. 2020. Association of American Railroads. Washington, DC.
2. Poudel, A. and M. Witte. November 2018. "Monitoring of Sub-Surface Fatigue Cracks in Railway Wheels using ACWDS." *Technology Digest* TD18-033. AAR/TTCI. Pueblo, CO.
3. Santos, R. et al., 2018. "New EMAT Solutions for the Railway Industry." ECNDT 2018. Gothenburg, Sweden.

For comments or questions about this publication, contact Anish_Poudel@aar.com